MINISTRY OF EDUCATION AND TRAINING

VIETNAM ACADEMY OF SCIENCE AND TECHNOLOGY

GRADUATE UNIVERSITY OF SCIENCE AND TECHNOLOGY

Pham Thu Thao

SELECTION OF APTAMERS FOR APPLICATION IN LATERAL FLOW IMMUNOASSAYS AND DIRECT ELISA FOR THE DETECTION OF *Pseudomonas aeruginosa* AND *Klebsiella pneumoniae*

SUMMARY OF DISSERTATION ON BIOLOGY

Major: Biochemistry

Code: 9 42 01 16

Hanoi – 2026

The dissertation is completed at: Graduate University of Science and Technology, Vietnam Academy Science and Technology

Supervisors:

1. Supervisor 1: Assoc. Prof. Dr. Truong Thi Ngoc Lien
2. Supervisor 2: Prof. Dr. Tran Dai Lam

Referee 1: Assoc. Prof. Dr. Nguyen Quang Huy

Referee 2: Dr. La Thi Huyen

The dissertation is examined by Examination Board of Graduate University of Science and Technology, Vietnam Academy of Science and Technology at…….. (time, date……)

The dissertation can be found at:

1. Graduate University of Science and Technology Library
2. National Library of Vietnam

LIST OF THE PUBLICATIONS RELATED TO THE DISSERTATION

1. **Pham, Thu Thao**, Thien-Kim Le, Nguyen TT Huyen, Nam Luyen Van, Tin Phan Nguy, Dai Lam Tran, and Lien Truong TN. "Staining-enhanced peroxidase-mimicking gold nanoparticles in nano-ELISA for highly sensitive detection of *Klebsiella pneumoniae*." *ACS omega* 8, no. 51 (2023): 49211-49217. https://doi.org/10.1021/acsomega.3c07503
2. **Pham, Thu Thao**, Nguyen TT Huyen, Lam Dai Tran, and TN Lien Truong. "Lateral flow immunoassay combined with color saturation for smartphone-based quantitative point-of-care detection of *Klebsiella pneumoniae*." *Advances in Natural Sciences: Nanoscience and Nanotechnology* 16, no. 1 (2025): 015016. DOI 10.1088/2043-6262/ada006
3. **Pham, Thu Thao**, Nguyen TT Huyen, Le Hong Oanh, Lam Dai Tran, Hiep V. Tran, TN Lien Truong, and Nguyen Thi Phuong Trang. "A Novel Aptamer Selection Strategy for *Pseudomonas aeruginosa* and Its Application as a Detecting Probe in a Nhanh Lateral Flow Assay." *Molecules* 30, no. 17 (2025): 3499. https://doi.org/10.3390/molecules30173499
4. Tran, Thuy-Duong Thi, Hai Ly Nguyen, Phan Thi Ngoc Hoa, **Thu Thao Pham**, Nguyen Thi Thanh Huyen, Giang Dau Huong, Hoa Thi Hoang et al. "Accelerated aptamer selection via SELEX and molecular simulations for lipopolysaccharide detection." *RSC advances* 15, no. 55 (2025): 46790-46806. DOI: 10.1039/D5RA06759F

INTRODUCTION

The World Health Organization (WHO) has stated that antimicrobial resistance in pathogenic bacteria is among the most serious challenges to global public health. Among the most prevalent multidrug-resistant (MDR) bacteria, as defined by the ESKAPE group, the two Gram-negative agents *Klebsiella pneumoniae* (KP) and *Pseudomonas aeruginosa* (PA) account for a substantial proportion of hospital-acquired infections. They are regarded by the United States Centers for Disease Control and Prevention (CDC) and WHO as urgent threats because of their rapid dissemination and persistent survival in the environment. Timely detection and accurate quantification of these microorganisms are important not only for clinical diagnosis but also as key factors in designing effective epidemiological control strategies.

In recent years, aptamers - short single-stranded DNA or RNA molecules (ssDNA/ssRNA) capable of binding specifically to targets with high affinity and selectivity - have emerged as a promising alternative to conventional antibodies. Owing to advantageous properties such as high thermal stability, ease of structural modification, and low production cost, aptamers are increasingly used in the development of next-generation biosensors. However, in Vietnam, studies on the selection of aptamers specific to local PA and KP bacterial strains remain limited. In particular, integrating these aptamers into modern diagnostic platforms, such as lateral flow immunoassay (LFIA) or one-step ELISA technology combined with nanomaterials to optimize rapid quantification, remains a challenging scientific problem.

Based on this practical demand, the dissertation entitled: “Selection of aptamers for application in lateral flow immunoassays and direct ELISA for the detection of *Pseudomonas aeruginosa* and *Klebsiella pneumoniae*” was conducted. The dissertation aims to establish aptamer selection technology while flexibly integrating immunological tools and nanomaterials to develop

highly sensitive detection systems, thereby contributing to the reduction of treatment costs and the improvement of medical diagnostic quality.

Research objectives of the dissertation:

- Select aptamer sequences with high affinity and specificity toward *Pseudomonas aeruginosa* and *Klebsiella pneumoniae*.
- Develop a direct ELISA technique that enables highly sensitive detection of *Pseudomonas aeruginosa* and *Klebsiella pneumoniae*.
- Develop an immunochromatographic technique that enables rapid and highly sensitive detection of *Pseudomonas aeruginosa* and *Klebsiella pneumoniae*.

Main research contents of the dissertation:

- Selection and affinity evaluation of aptamers specific to *P. aeruginosa* and *K. pneumoniae.*
- Development of a direct ELISA technique based on biorecognition conjugates and gold nanoparticles for the detection of *Pseudomonas aeruginosa* and *Klebsiella pneumoniae*.
- Design and fabrication of lateral flow immunoassay (LFIA) test strips for the rapid detection of *Pseudomonas aeruginosa* and *Klebsiella pneumoniae*.

CHAPTER 1. OVERVIEW

1.1. Hospital-acquired infections and the two target pathogens *Pseudomonas aeruginosa* and *Klebsiella pneumoniae*

Hospital-acquired infections (HAIs) are an important cause of increased morbidity and mortality, prolonged hospitalization, and substantial economic burden, particularly in intensive care units and in low- and middle-income countries. Common HAI agents include various Gram-positive and Gram-negative bacteria, among which *Pseudomonas aeruginosa* and *Klebsiella pneumoniae* play prominent roles. Antimicrobial resistance, especially carbapenem resistance among WHO-priority bacteria, has been increasing markedly in Vietnam, creating an urgent need to strengthen surveillance, diagnosis, and the development of new therapeutic strategies.

1.2. Aptamers as promising bioreceptors in bacterial diagnostics

Aptamers are synthetic bioreceptors with high specificity and affinity for their targets, selected through SELEX (Systematic Evolution of Ligands by Exponential Enrichment) strategies and variants of this technique. Compared with antibodies, aptamers offer notable advantages, including artificial synthesis, high stability, ease of chemical modification, and low cost. Owing to these properties, aptamers have been increasingly applied in the development of biosensors and rapid immunoassays. Therefore, aptamers are regarded as a highly promising approach for the rapid diagnosis of bacteria associated with hospital-acquired infections.

1.3. Development trends in rapid bacterial detection methods based on LFIA and nano-ELISA

LFIA is a rapid testing technique based on the combination of capillary chromatographic flow and specific biochemical reactions, using antibodies or nucleic acids, such as aptamers, as biorecognition probes. A typical LFIA strip consists of four main components: the sample pad, conjugate pad,

nitrocellulose membrane, and absorbent pad, each serving a distinct role in maintaining stable flow and specific reactions. LFIA is commonly implemented in two formats: sandwich assays for large molecules and competitive assays for small molecules, with different signal-generation mechanisms used to determine positive or negative results. Labeling materials in LFIA are diverse; gold nanoparticles are the most widely used because of their distinctive optical properties, high stability, and visibility to the naked eye. In parallel with LFIA, the development of nano-ELISA using nanozymes and gold nanoparticles as alternatives to conventional enzymes has demonstrated superior potential for enhancing the sensitivity, specificity, and applicability of modern immunoassays.

CHAPTER 2. MATERIALS AND METHODS

2.1. Research subjects, materials and equiqment

The research subjects consisted of two bacterial strains associated with hospital-acquired infections, *Pseudomonas aeruginosa* and *Klebsiella pneumoniae* (inactivated), as well as other bacterial strains used to evaluate aptamer specificity.

Materials and chemicals for aptamer selection included a random ssDNA library, biotin/FAM-labeled primer systems, streptavidin magnetic beads, buffer solutions for the SELEX selection process, PCR reagents, and DNA purification kits. In addition, materials for developing the lateral flow immunoassay (LFIA), nano-ELISA, and gold nanoparticle (AuNP) synthesis included strip assembly membranes, buffer components, TMB, and H_2O_2. The main instruments included PCR systems, UV–Vis spectrophotometers, Zetasizer, TEM, and microbiological culture equipment.

2.2. Selection of aptamers specific to *Klebsiella pneumoniae*

The aptamer selection procedure was performed using an accelerated SELEX method comprising three main stages. The pre-selection stage focused on designing an ssDNA library containing a 55-nucleotide random region to ensure a balance between structural diversity and specific binding capability. The primer system was designed to avoid dimer formation and to ensure high PCR efficiency. The DNA library was immobilized and ssDNA was separated using streptavidin magnetic beads through biotin–streptavidin binding. The accelerated SELEX stage was conducted on ELISA plates coated with *K. pneumoniae* antigen - LPS. Aptamer enrichment was monitored by quantifying ssDNA before and after selection, combined with agarose gel electrophoresis and PCR. After the final selection round, aptamer sequences were amplified, cloned, sequenced, and analyzed

bioinformatically. Representative sequences were selected based on occurrence frequency and secondary-structure stability.

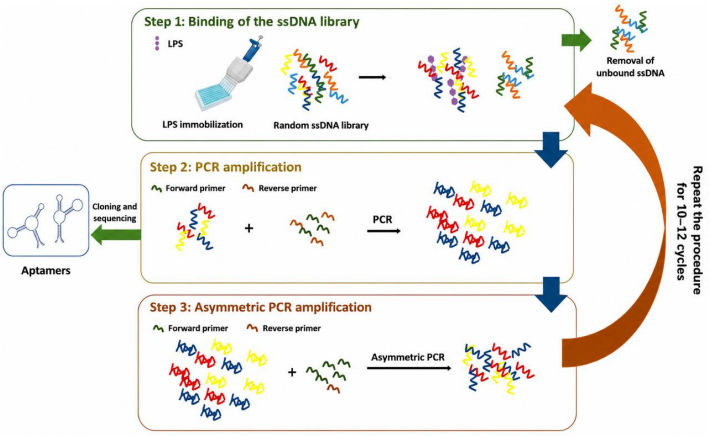

Figure 2.1. Aptamer selection workflow for *Klebsiella pneumoniae* antigen.

The secondary and tertiary structures of the aptamers were predicted using mFold and RNAComposer, converted into DNA form, and subjected to energy optimization. Interactions between aptamers and lipopolysaccharide (LPS) from *K. pneumoniae* were investigated by molecular docking and molecular dynamics simulations. Parameters such as RMSD, RMSF, hydrogen bonds, and binding free energy were used to evaluate the stability of the aptamer–LPS complexes. In parallel, experimental techniques including ELONA, SERS, electrochemical impedance spectroscopy (EIS), and differential pulse voltammetry (DPV) were used to confirm specific interactions and determine the dissociation constant (Kd) of the aptamers.

2.3. Selection of aptamers specific to *Pseudomonas aeruginosa*

The SELEX procedure for *P. aeruginosa* was conducted using a cell-SELEX approach, in which the ssDNA library was incubated directly with inactivated bacterial cells. Specifically bound aptamers were recovered after washing and thermal release, followed by amplification using PCR and

asymmetric PCR. The stringency of selection was gradually increased over successive rounds. The resulting aptamers were sequenced, structurally analyzed, and evaluated for specificity against other bacterial strains.

2.4. Direct ELISA procedure for detecting *Klebsiella pneumoniae* and *Pseudomonas aeruginosa*

Klebsiella pneumoniae and *Pseudomonas aeruginosa* at different concentrations were immobilized on polystyrene plates. The assay then proceeded through blocking, incubation with AuNP–antibody conjugates for *Klebsiella pneumoniae* or AuNP–aptamer conjugates for *Pseudomonas aeruginosa*, staining enhancement using $HAuCl_4/NH_2OH{\cdot}HCl$, and color development with TMB/H_2O_2. The signal was measured at 650 nm. The sensitivity, limit of detection (LoD), limit of quantification (LoQ), and specificity of the method were determined using negative samples and control bacterial strains.

2.5. Fabrication of LFIA rapid test strips for *Klebsiella pneumoniae* detection

The LFIA strips were designed according to the immunological sandwich principle and consisted of four main components: sample pad, conjugate pad, nitrocellulose membrane, and absorbent pad. The membranes were treated with suitable buffer systems to ensure stable capillary flow and to reduce background interference. Rabbit anti-*Klebsiella pneumoniae* polyclonal antibodies and Mouse anti-rabbit IgG antibodies were sprayed onto the test line (T) and control line (C), respectively. Test results were read after 15 minutes and quantified by measuring the color saturation of the test line using a smartphone camera combined with a color-analysis application.

2.6. Fabrication of LFIA rapid test strips for *Pseudomonas aeruginosa* detection

The rapid test strip for *Pseudomonas aeruginosa* operates based on a dual aptamer–antibody conjugation principle to improve assay specificity and reliability. During sample preparation, the specific aptamer was attached to gold nanoparticles to form an AuNP–aptamer probe capable of selectively recognizing and binding the target bacteria in the sample. When a bacteria-containing sample is applied to the strip, the AuNP–aptamer–bacterium complex migrates by capillary flow along the nitrocellulose membrane and is captured at the T line by immobilized specific antibodies. In parallel, the AuNP–Goat anti-mouse IgG antibody system preloaded in the conjugate region migrates and is retained at the C line through immunological interaction with Mouse anti-rabbit IgG antibodies. Images of the test line (T) and control line (C) regions on the LFIA strips were processed using ImageJ software to quantify color signal intensity.

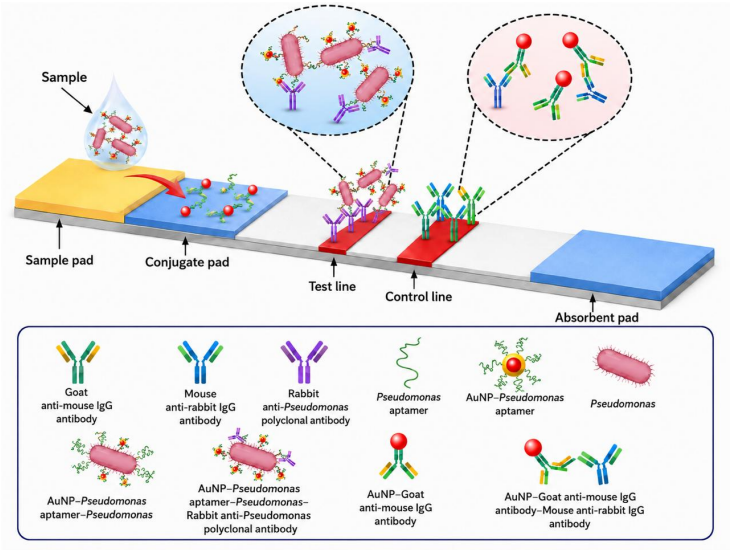

Figure 2.2. Schematic principle of an aptamer-based rapid test strip using a dual-conjugate system for *Pseudomonas aeruginosa* detection.

CHƯƠNG 3. RESULTS AND DISCUSSION

3.1. Characterization of gold nanoparticles

Colloidal AuNPs were successfully synthesized as a monodisperse suspension using the standard citrate reduction method. In this study, the synthesized spherical gold nanoparticles had an average size of 15 ± 2 nm. Their morphology and physicochemical properties were clearly confirmed by DLS analysis and TEM imaging (**Figure 3.1**). The UV–Vis absorption spectrum of the AuNPs displayed a characteristic peak at approximately 520 nm, and their zeta potential was −21.85 mV (**Figure 3.1**). These results indicate that the synthesized AuNPs possessed the desired characteristics, including uniform size, spherical morphology, and negative surface charge, which are highly suitable for biomolecular techniques.

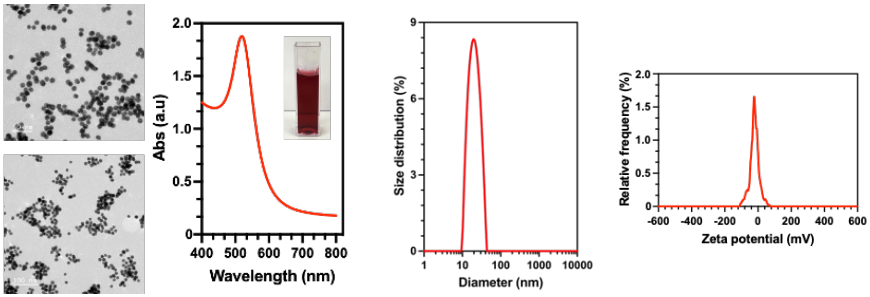

Figure 3.1. TEM images at 50 nm and 100 nm scale bars and UV–Vis spectrum from 400 to 800 nm of AuNPs. Dynamic light scattering (DLS) measurements show the hydrodynamic diameter and zeta potential of the gold nanoparticles.

3.2. Selection of aptamers specific to *Klebsiella pneumoniae*

In this *in vitro* SELEX procedure, LPS from *Klebsiella pneumoniae* was used as the target for a random ssDNA library consisting of 455 ssDNA molecules. After ten selection rounds, a pool of aptamers with markedly improved binding affinity toward LPS was successfully obtained.

Enrichment was clearly demonstrated by an enzyme-linked oligonucleotide assay: while the initial library showed only a weak absorbance signal at 450 nm, the signal intensity increased substantially from round 8 onward and almost reached saturation by round 10 (**Figure 3.2**).

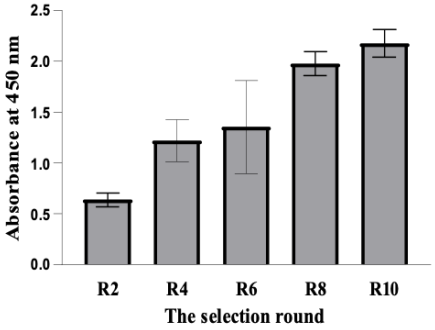

Figure 3.2. Enrichment of the aptamer library specific to LPS from *Klebsiella pneumoniae* during SELEX.

To support the experimental SELEX results, a systematic computational screening workflow was established, including molecular docking, molecular dynamics (MD) simulations, and coordination number (CN) analysis. The combined docking results indicated that aptamers No.5, No.7, and No.9 were promising candidates, showing a favorable balance between binding energy and characteristic interaction profiles.

After docking configurations had been obtained, molecular dynamics (MD) simulations were performed to evaluate the stability and energetically favorable conformations of the aptamer–LPS complexes. This workflow showed that binding affinity cannot be inferred from a single parameter alone, such as docking energy or the number of hydrogen bonds, but rather results from complex interactions among van der Waals forces, electrostatics, solvation, and entropy effects. The results showed that although aptamer No.9 displayed advantages in contact frequency and structural stability,

aptamer No.5 achieved more favorable binding free energy and experimentally confirmed recognition performance (**Table 3.1**).

Table 3.1. Three-dimensional structures of the selected aptamer–LPS complexes (No.5, No.7, and No.9) and hydrogen bonds between aptamer residues and LPS.

Aptamer sequence	Aptamer–LPS complex structure	Hydrogen bonds	Energy (kcal/mol)
No.5	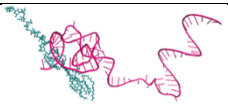	T26 – KPLI (2 bonds) T24 – KPLI G5 – BGA6	- 50,13
No.7	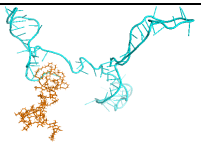	T61 – AHE4 G60 – BGL5 T44 – AKD12	- 49,3
No.9	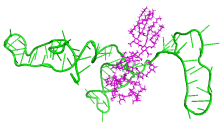	T29 – BGA16 G57 – BGL11 G58 – AGA10 G61 – AKD2	- 44,27

SERS results showed that only aptamer No.5 exhibited clear spectral changes characteristic of specific binding to LPS, whereas aptamer No.7 and aptamer No.9 did not show similar changes. This difference suggests that although all three aptamers may bind to LPS through electrostatic interactions, only aptamer No.5 forms a structurally stable and favorable interaction (**Figure 3.3**). Changes in electrical impedance were recorded during binding to LPS. Specifically, aptamer No.5 showed a marked increase in impedance, whereas aptamer No.7 exhibited a decreasing impedance trend. In contrast, the impedance response of aptamer No.9 changed very little in the presence of LPS, indicating weak interaction. These results suggest that

among the tested sequences, aptamer No.5 possesses the strongest and most stable binding affinity toward LPS, whereas aptamer No.7 shows an atypical response and aptamer No.9 exhibits very low affinity (**Figure 3.4**).

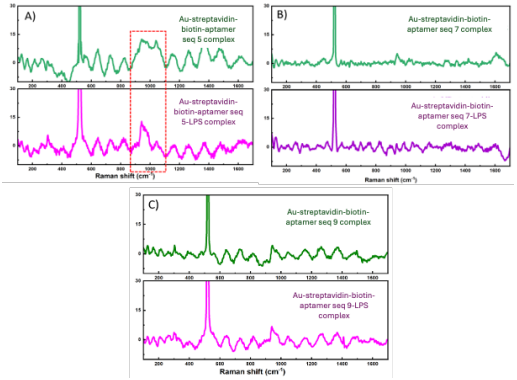

Figure 3.3. Surface-enhanced Raman scattering (SERS) spectra of selected aptamers before and after interaction with LPS from *Klebsiella pneumoniae.*

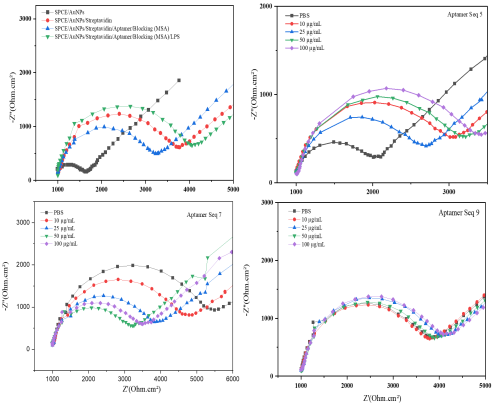

Figure 3.4. (A) Schematic mechanism of electrochemical impedance spectroscopy (EIS). (B–D) Nyquist plots of electrodes immobilized with aptamers No.5, No.7, and No.9 after exposure to different concentrations of LPS from *Klebsiella pneumoniae* (10, 25, 50, and 100 µg/mL), showing concentration-dependent impedance responses.

3.3. Selection of aptamers specific to *Pseudomonas aeruginosa*

The concentration of single-stranded DNA (ssDNA) obtained after each SELEX round increased over time, indicating enrichment of sequences with higher binding affinity toward *P. aeruginosa* (**Figure 3.5**). Details of the aptamer selection process, including docking scores, 2D/3D structural models, and docking interaction images, are presented in **Table 3.2**.

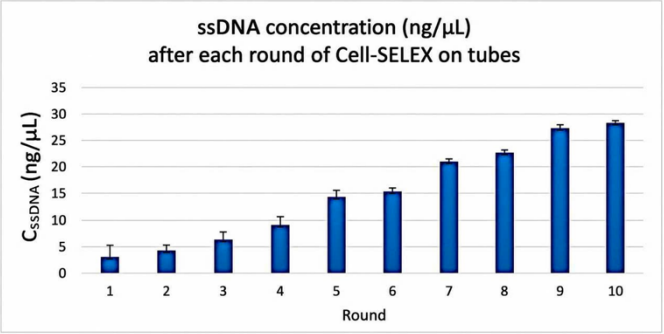

Figure 3.5. Changes in ssDNA concentration across cell-SELEX rounds for *P. aeruginosa*

After ten rounds of cell-SELEX and counter-selection against *E. coli* and *K. pneumoniae* to eliminate nonspecific binding sequences, the enriched aptamer population was cloned using the TOPO TA Cloning® kit. Sixteen white colonies were selected, followed by plasmid extraction and Sanger sequencing using the universal M13 primer. Sequence analysis revealed six dominant aptamer sequences, indicating convergence toward specific binding motifs. These six representative sequences were further analyzed for secondary structure using Mfold [137], [138] and for molecular binding affinity using HDOCK [139] with the LPS region on the surface of *P. aeruginosa.*

Table 3.2. Characteristics of selected aptamers, including nucleotide sequence, docking score, predicted minimum free energy (ΔG), frequency (%), diversity score, and corresponding 2D, 3D, and molecular docking (MD)

configurations constructed from the minimum free energy (MFE) model of the six selected aptamers.

Aptamer Name	Aptamer DNA Sequence	Docking Score	MFE (kcal/mol)	Frequency (%)	Diversity Score	Predicted Secondary Structure (2D) Based on MFE Model	Predicted Tertiary Structure (3D) Based on MFE Model	Molecular Docking with CPA
T1	ATCCGTCACACCTGCTCTGTAAACACCTAC-GGTCTTAGCATACGGTATAAGCCGTAAC-CGGTTTTACCTAAACTGGTGTTGGCTCCCGTAT	−453.85	−27.10	24.98	4.64			
T2	ATCCGTCACACCTGCTCTCAAAGGTCATA-CGGCCTTCTTGGCAGCGTAATGCCTTGC-TCGCATTTTTCCCTCATGGTGTTGGCTCCCGTAT	−366.23	−22.11	3.82	28.74			
T3	ATCCGTCACACCTGCTCTCATCATGCC-CGCGTTCTAATAACTGCTATATCCTTTAT-CGCCTCTATCCCTCCGTGGTGTTGGCTCCCGTAT	−409.72	−12.20	8.83	13.74			

Among the six selected aptamers, aptamer T1 was the most frequently detected sequence (appearing in 4 of 16 colonies). It exhibited the highest MFE-structure frequency, the lowest diversity score, and the most favorable docking score with CPA of *P. aeruginosa*.

3.4. Development of direct ELISA for detecting *Klebsiella pneumoniae* and *Pseudomonas aeruginosa*

Gold nanoparticles were investigated as peroxidase-like catalysts, and TMB was used as a substrate capable of producing a blue color in the presence of H_2O_2. Nanozyme activity reached the highest efficiency with 0.02 mg TMB and 150 µL H_2O_2, as the strongest blue color was observed at these conditions after 30 minutes of incubation. In this study, the concentrations of $HAuCl_4$ and $NH_2OH{\cdot}HCl$ were optimized for the staining-enhancement procedure. Nanozyme activity produced the highest signal at 2 mM $HAuCl_4$ and 10 mM $NH_2OH{\cdot}HCl$. **Figure 3.6** shows that staining-enhanced AuNPs exhibited significantly higher activity than unstained AuNPs, with an

approximately threefold statistically significant increase. These results demonstrate that the nanozyme exhibits improved activity after staining enhancement, confirming the feasibility of using the staining-enhancement strategy.

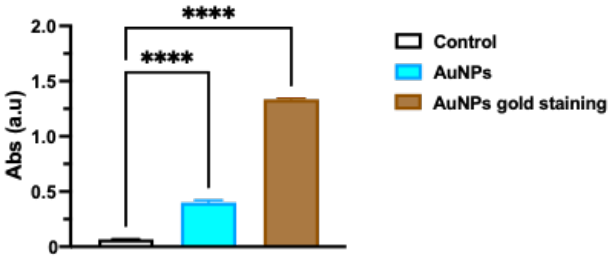

Figure 3.6. Evaluation of nanozyme activity of AuNPs and staining-enhanced AuNPs measured by absorbance at 650 nm.

With staining enhancement, the threshold value was higher at 0.158 (Figure 3.7), indicating that samples with OD values above 0.158 were considered positive, whereas samples below this value were considered negative. Staining-enhanced nano-ELISA was investigated by measuring OD_{650} for the detection of *Klebsiella pneumoniae* from 10^1 to 10^8 CFU/mL (Figure 3.8). The linear regression equation was determined as $y = 0.1559\log10(x) - 0.1048$. The curve showed a strong positive correlation between *Klebsiella pneumoniae* concentration (CFU/mL) and OD_{650} signal ($R^2 = 0.9699$). The LoD and LoQ were calculated as 36.230 and 78.857 CFU/mL, respectively. Staining-enhanced nano-ELISA could detect concentrations as low as 10^2 CFU/mL, which is 100-fold more sensitive than nano-ELISA using AuNPs without staining enhancement.

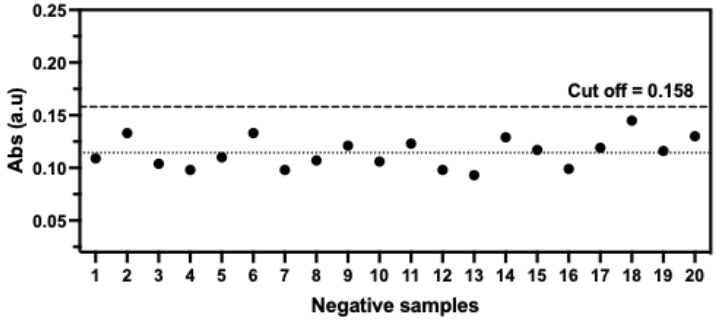

Figure 3.7. Determination of the threshold value for staining-enhanced nano-ELISA.

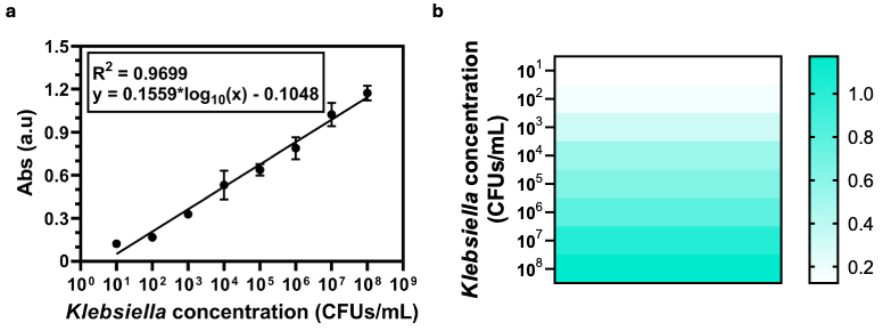

Figure 3.8. Linear calibration of *Klebsiella pneumoniae* with serial dilutions from 10^1 to 10^8 CFU/mL: (a) calibration curve and (b) blue color heat map of the *Klebsiella pneumoniae* detection range in staining-enhanced nano-ELISA.

The sensitivity and linear response range of the nano-ELISA assay were investigated by measuring OD_{650} for the detection of *P. aeruginosa* from 10^1 to 10^9 CFU/mL (**Figure 3.9**). The linear regression equation was determined as y = 0.0997log10(x) + 0.0341. The curve showed a strong positive correlation between *P. aeruginosa* concentration (CFU/mL) and OD_{650} signal (R^2 = 0.9828). The LoD and LoQ were calculated as 26.795 and 88.423 CFU/mL, respectively.

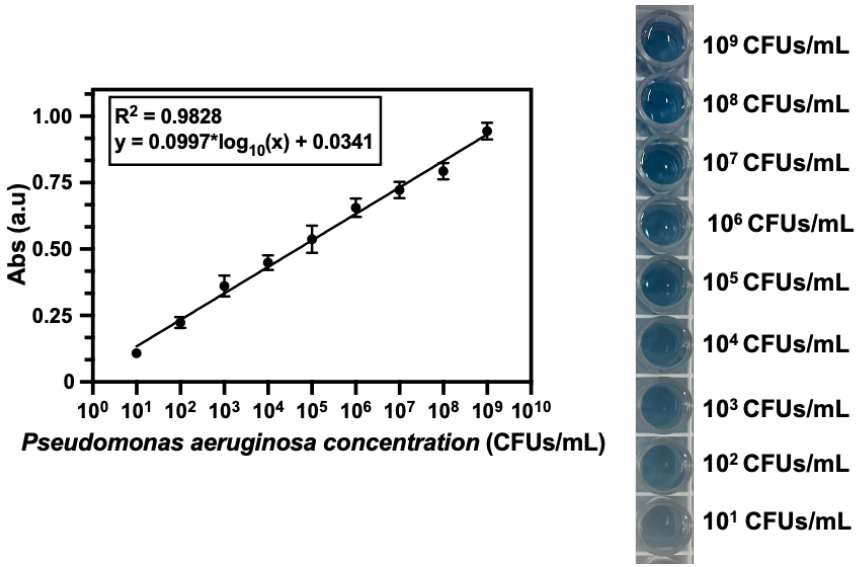

Figure 3.9. Linear calibration of *P. aeruginosa* with serial dilutions from 10^1 to 10^9 CFU/mL. The post-reaction solution showed a blue color gradient from dark to light, proportional to bacterial concentration in nano-ELISA.

3.5. LFIA rapid test strip for *Klebsiella pneumoniae* detection

In this study, a covalent coupling method was applied to attach functional groups to the AuNP surface through the EDC/NHS reaction. The shift in the UV–Vis absorption peak (**Figure 3.10C**) demonstrated that AuNP functionalization with the MUA ligand effectively linked to the Kleb Ab antibody molecule. The zeta potential of AuNPs decreased from −38.38 mV to −0.15 mV (**Figure 3.10B**), reflecting reduced negative charge due to binding of positively charged antibody molecules. In addition, particle size increased after covalent conjugation (**Figure 3.10A**), confirming coverage of the AuNP surface by antibody molecules.

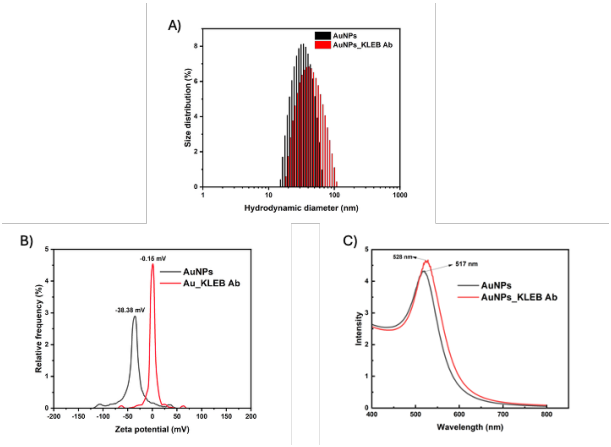

Figure 3.10. (A) Hydrodynamic size, (B) zeta potential, and (C) UV–Vis absorption spectra from 400 to 800 nm of gold nanoparticles (AuNPs) and AuNP–*Klebsiella pneumoniae* antibody complexes.

LFIA strips were fabricated and evaluated for their ability to detect Klebsiella pneumoniae over a concentration range from 10^1 to 10^8 CFU/mL (**Figure 3.11**). The detection line for Klebsiella pneumoniae could be clearly observed at 10^2 CFU/mL. The sensitivity and calibration range of the LFIA strip integrated with the color-saturation analysis system were evaluated based on the intensity of the detection line across concentrations from 10^1 to 10^8 CFU/mL.

(A)

(B)

Figure 3.11. (A) The LFIA test strip was evaluated for its ability to detect *K. pneumoniae* over a concentration range of 10^1 to 10^8 CFU/mL. (B) Images of the LFIA test strips were captured under illumination at an illuminance of 335 lux.

The R, G, and B values in the RGB model were used to determine the intensity and color saturation at the LFIA test line (T line). The linear regression equation was determined as y = 2.983 + 3.285log10(x). The regression showed a high correlation between *Klebsiella pneumoniae* concentration and color-saturation signal, with $R^2 = 0.995$ (**Figure 3.12**). The limits of detection (LoD) and quantification (LoQ) were calculated as 1.61 and 4.83 CFU/mL, respectively.

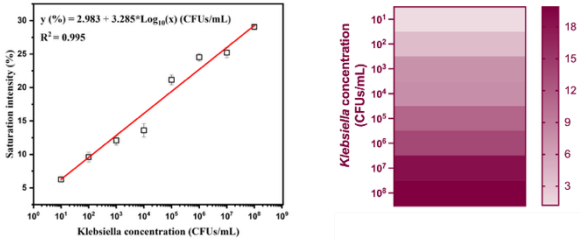

Figure 3.12. (A) Calibration curve and (B) pink-scale heat map of *Klebsiella pneumoniae* with serial dilutions from 10^1 to 10^8 CFU/mL.

Specificity experiments showed no false-positive signal on test strips challenged with *E. coli* and *P. aeruginosa* by naked-eye observation (**Figure 3.13**), demonstrating that the developed quantitative LFIA system possesses high specificity, strong resistance to interference, and accurate detection capability for *Klebsiella pneumoniae*.

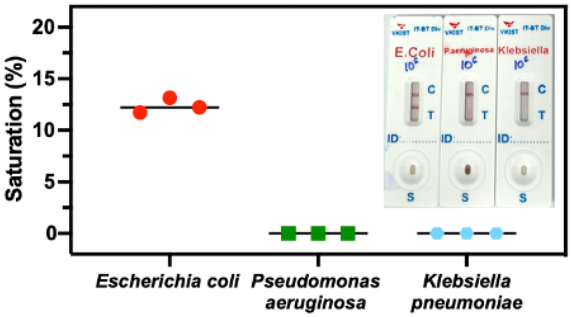

Figure 3.13. Specificity analysis of the test strip for detecting *K. pneumoniae*, *Escherichia coli*, and *P. aeruginosa* at 10^8 CFU/mL.

3.6. LFIA rapid test strip for *Pseudomonas aeruginosa* detection

To evaluate the specificity of the LFIA strip, blank buffer samples and suspensions of nontarget bacteria, including *E. coli*, *K. pneumoniae*, and *S. aureus*, produced only the C line and no signal at the T-line position (**Figure 3.14**).

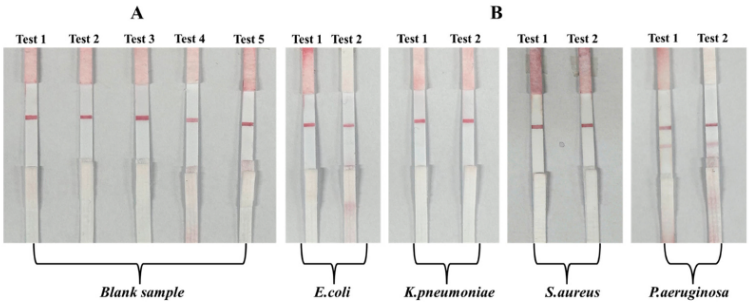

Figure 3.14. Specificity evaluation using blank samples, *E. coli*, *K. pneumoniae*, *S. aureus*, and *P. aeruginosa*.

To determine sensitivity, positive samples containing *P. aeruginosa* in the range from 5×10^2 to 10^9 CFU/mL produced both the control line (C) and the test line (T), with the intensity of the T line varying according to bacterial concentration (**Figure 3.15**).

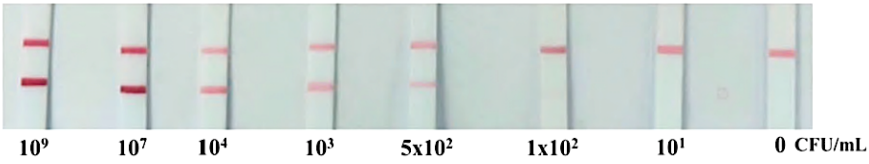

Figure 3.15. LFIA strip results at different concentrations of *P. aeruginosa*

For semi-quantitative analysis, images of the test region (T) and control region (C) on the LFIA strips were processed using ImageJ software. The calibration curve obtained from LFIA strips using samples spiked with P. aeruginosa showed a strong linear relationship between test-line intensity (y) and bacterial concentration (x) in the range from 10^1 to 10^9 CFU/mL, described by the equation y = 9.858x + 67.717, with a very high correlation coefficient ($R^2 = 0.993$) (**Figure 3.16**).

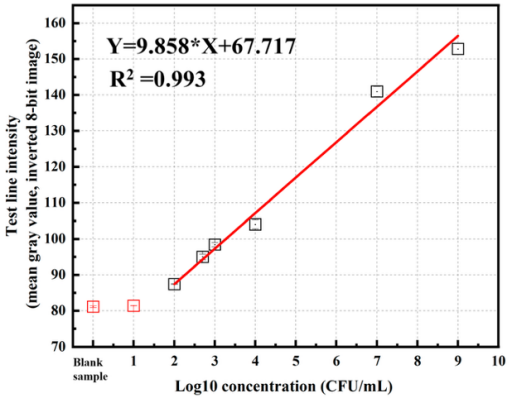

Figure 3.16. Calibration curve showing the relationship between test-line (T-line) intensity and *P. aeruginosa* concentration in the sample.

CONCLUSIONS AND RECOMENDATIONS

CONCLUSIONS

1. A total of 15 potential aptamers specific to *K. pneumoniae* and 6 potential aptamers specific to *P. aeruginosa* were screened using the SELEX method. Based on in silico analysis, aptamer No. 5 and aptamer T1 were subsequently selected as the most promising aptamers specific to *K. pneumoniae* and *P. aeruginosa*, respectively.
2. The dissertation developed a direct ELISA system based on the successful conjugation of gold nanoparticles with Rabbit anti-*K. pneumoniae* polyclonal antibody. Optimization of the staining method in the presence of $HAuCl_4$ and $NH_2OH{\cdot}HCl$ increased the detection sensitivity 100-fold, enabling the detection of *K. pneumoniae* at a low concentration of 10^2 CFU/mL.
3. The dissertation developed a direct ELISA system based on the successful conjugation of gold nanoparticles with aptamer T1 for the detection of *P. aeruginosa* at a low concentration of 10^2 CFU/mL.
4. A rapid LFIA test strip was developed based on the successful conjugation of Rabbit anti-*K. pneumoniae* polyclonal antibody onto the surface of gold nanoparticles for direct use as the secondary antibody in the LFIA test strip. The test strip enabled the detection of *K. pneumoniae* at a concentration of 10^1 CFU/mL and showed no cross-reactivity with *E. coli*, *S. typhimurium*, *C. perfringens*, *S. aureus*, or *P. aeruginosa*.
5. A rapid LFIA test strip for the detection of *P. aeruginosa* was developed based on the successful adsorption of aptamer T1 onto the surface of gold nanoparticles, serving similarly to a specific secondary antibody. The test strip exhibited an experimentally determined low limit of detection for *P. aeruginosa* at 2.34×10^2 CFU/mL and showed no cross-reactivity with *E. coli*, *S. typhimurium*, *C. perfringens*, *S. aureus*, or *K. pneumoniae*.

RECOMENDATIONS

1. Conduct testing of the detection system on real clinical samples to evaluate applicability under complex specimen conditions.

2. Expand the number of samples with a larger scale and more diverse specimen origins to comprehensively evaluate the specificity of the selected aptamers and to determine potential cross-reactivity with species within the same genera, such as *Klebsiella* and *Pseudomonas*, or other microorganisms commonly encountered in hospital-acquired infections.

3. Perform testing on clinical specimens with different bacterial loads to evaluate the practical sensitivity of the detection system, particularly in cases with low bacterial concentrations during the early stage of infection.

4. Continue optimizing reaction conditions and fabrication procedures for immunochromatographic test strips and direct ELISA to improve system stability, reproducibility, and storage capacity.

NOVEL CONTRIBUTIONS OF THE DISSERTATION

- The dissertation developed an effective screening workflow for aptamers specific to two bacterial species frequently associated with severe hospital-acquired infections, namely *Pseudomonas aeruginosa* and *Klebsiella pneumoniae*.
- The dissertation demonstrated the effectiveness of using gold nanoparticle-conjugated aptamers as specific secondary antibody analogues in rapid immunochromatographic strips and direct ELISA.
- The dissertation demonstrated the application potential of combining diverse biorecognition components, such as aptamers and antibodies, with gold nanomaterials to construct integrated diagnostic platforms, including lateral flow immunoassay (LFIA) and nano-ELISA, thereby enhancing rapid screening capability with high sensitivity for *Pseudomonas aeruginosa* and *Klebsiella pneumoniae*.